Talanta 116 (2013) 199–204

Contents lists available at ScienceDirect

Talanta

journal homepage: www.elsevier.com/locate/talanta

Ultra-sensitive non-aggregation colorimetric sensor for detection of iron based on the signal amplification effect of Fe^{3+} catalyzing H_2O_2 oxidize gold nanorods

Jia-Ming Liu [a,*], Xin-Xing Wang [a], Li Jiao [a], Ma-Lin Cui [a], Li-Ping Lin [a], Li-Hong Zhang [b], Shu-Lian Jiang [c]

[a] Department of Chemistry and Environmental Science, Zhangzhou Normal College, Zhangzhou 363000, PR China
[b] Department of Food and Biological Engineering, Zhangzhou Institute of Technology, Zhangzhou 363000, PR China
[c] Fujian provincial bureau of quality and technical supervision, Zhangzhou 363000, PR China

ARTICLE INFO

Article history:
Received 8 March 2013
Received in revised form
6 May 2013
Accepted 11 May 2013
Available online 16 May 2013

Keywords:
Gold nanorods
Longitudinal plasmon absorption band
Signal amplification
Catalyzing non-aggregation colorimetric sensor
Iron

ABSTRACT

Fe^{3+} can catalyze H_2O_2 to oxidize along on the longitudinal axis of gold nanorods (AuNRs), which caused the aspect ratio of AuNRs to decrease, longitudinal plasmon absorption band (LPAB) of AuNRs to blueshift ($\Delta\lambda$) and the color of the solution to change obviously. Thus, a rapid response and highly sensitive non-aggregation colorimetric sensor for the determination of Fe^{3+} has been developed based on the signal amplification effect of catalyzing H_2O_2 to oxidize AuNRs. This simple and selective sensor with a wide linear range of 0.20–30.00 μM has been utilized to detect Fe^{3+} in blood samples, and the results consisted with those obtained by inductively coupled plasma-mass spectroscopy (ICP–MS). Simultaneously, the mechanism of colorimetric sensor for the detection of Fe^{3+} was also discussed.

1. Introduction

As one of the essential trace elements, iron plays a key role in human body on the progress of physiology and biochemistry. Iron deficiency may lead to low immunity and infectious diseases, while the human body takes in too much iron, it will cause excretory functional disturbance and likely have greater carcinogenic potential [1]. On the other hand, it is well known that iron is one of the lower toxic elements in the environment appearing in various natural waters. So it is very necessary to develop fast, accurate and sensitive methods for the determination of trace iron in different samples such as water, food, medicaments and biochemical materials. In recent years, many methods have been reported for the determination of Fe^{3+}, such as atomic absorption spectrometry (The limit of detection (LOD) is 0.032 μM [2], voltammetry [3], ICP–MS [4,5], and inductively coupled plasma-atomic emission spectrometry (LOD is 0.47 μM.) [6]. However, most of these methods are complicated because they need derivatization, expensive equipment and combination with various detection methods. In addition, their sensitivities are low and liner ranges are narrow. However, the catalytic–kinetic methods and colorimetric sensor for the determination of iron have received considerable attention because of its high sensitivity and accuracy without expensive and special apparatus.

Tracing the developing frontier of science and technology, research results of nanotechnology and nanomaterials in analysis of biological and pharmaceutical samples aroused great attentions. Recently, variety of nanomaterials have been used as electrochemical sensor in the determination of the bioactive substances, such as carbon nanotube [7–9], ionic liquid/multiwall carbon nanotube [10,11], multiwall carbon nanotubes [12,13], Ag nanoparticles [14] and so on, showing a broad application prospect of nanomaterials. But the application of these nanomaterials was limited for their drawbacks. For example, carbon nanotube will be dissolved in water only if their surfaces have been modified.

In order to overcome these shortcomings, Wu et al. have developed a sensitive and selective colorimetric detection of Fe^{3+} using pyrophosphate functionalized gold nanoparticles [15]. Compared with gold nanoparticles, much more attention has been focused on AuNRs due to unique optical properties, which is mainly attributed to the fact that AuNRs possess two plasmon absorption bands: LPAB and transverse plasmon absorption band (TPAB) [16]. Thereinto, the location of LPAB mainly depends on the shape, surface charge, and dielectric condition of AuNRs and keeps

* Corresponding author. Tel.: +86 596 2591352.
E-mail address: zzsyliujiaming@126.com (J.-M. Liu).

0039-9140/$ - see front matter © 2013 Elsevier B.V. All rights reserved.
http://dx.doi.org/10.1016/j.talanta.2013.05.024

mostly unchangeable [17]. In recent years, a lot of colorimetric sensors of AuNRs have been developed based on the change of LPAB [18], such as the determination of Hg (II) [19], Cr (VI) [20], NO_2^- [21], cysteine [22] and glutathione [23], showing its remarkable practicality. The AuNRs have been the effective and direct ways to increase the sensitivity of colorimetric sensor. A catalyzing non-aggregation colorimetric sensor for the determination of Fe^{3+} has been developed based on the combination of catalytic reaction and colorimetric sensor due to the amplification effect of catalytic reaction could enhance visual signals, which would further improve the selectivity and sensitivity of colorimetric sensor.

In this paper, it was observed that Fe^{3+} can catalyze H_2O_2 to oxidize along on the longitudinal axis of AuNRs in HCl medium (pH=1.55) at 70 °C for 25 min, which caused the aspect ratio of AuNRs to decrease and the $\Delta\lambda$ of system to increase sharply as well as the color of the solution to change obviously, showing Fe^{3+} has signal amplification effect on the $\Delta\lambda$ of system. Based on the above phenomena, a rapid response and highly sensitive non-aggregation colorimetric sensor toward Fe^{3+} was developed. Compared with gold nanoparticles colorimetric sensor [15], the linear range of catalyzing colorimetric sensor is 25 times wider, and its LOD is 84 times lower, indicating that the sensor was suitable for the Fe^{3+} detection in real samples with wider linear range and low content. To our knowledge, non-aggregation colorimetric sensor for the determination of Fe^{3+} based on the signal amplification effect of catalyzing H_2O_2 to oxidize AuNRs has not been reported yet. This study not only provides a new way for the design of colorimetric sensor and improves the sensitivity of colorimetric sensor, but also promotes the applications of AuNRs and development of trace analysis.

2. Experimental section

2.1. Instrumentation and chemicals

Absorbance measurements were carried out on using a Shimadzu UV-2550 spectrophotometer with one pair of 10-mm quartz cell. The membrane filter (0.45 μm pore size) was used for the filtration of blood samples. ICP–MS analysis was performed in this experiment (Agilent 7500, USA).

Fe^{3+} working solution: 1.00 mg mL^{-1} Fe^{3+} standard solution (GSBG 62020–90 2601, China National Analysis and Testing Centre for Iron and Steel) was diluted to 10.0 μM. $HAuCl_4 \cdot 3H_2O$ (> 99%), $AgNO_3$ (> 99%), $NaBH_4$ (99%), L-ascorbic acid (> 99%), cetyltriethylammnonium bromide (CTAB, > 99%) and H_2O_2 (30%) were from Sinopharm Chemical Reagent Co., Ltd (Shanghai, China). Nanopure deionized and distilled water (18.2 MΩ) was used in all experiments.

2.2. Synthesis of AuNRs

AuNRs were synthesized according to silver ion-assisted seed-mediated method previously reported by El-Sayed and co-workers [24].

Briefly, 5.00 mL of 0.20 M CTAB was mixed with 5.00 mL of 0.020 mM $HAuCl_4$ and stirred vigorously. Thereafter, 0.60 mL of 0.010 M $NaBH_4$ (ice-cold) was added, and the color of the solution changed from dark yellow to brownish yellow under vigorous stirring, indicating the formation of seed solution. The seed solution was kept in a water bath at 28 °C for at least 2 h before use.

In a flask, 75.00 mL of 0.20 M CTAB was mixed with 1.25 mL of 4 mM $AgNO_3$ solution and 75.00 mL of 1.0 mM $HAuCl_4$. Then, 1.05 mL of 0.10 M L–ascorbic acid (> 99%) was added and the growth solution was obtained. With continuously stirring this mixture, 180 μL seed solution was taken out and added to AuNRs growth solution at 28 °C. The color of the solution gradually changed to red in the first 15 min until finally stabilized. The solution was aged at 28 °C for 24 h to ensure full growth of AuNRs.

2.3. Colorimetric assay

1.50 mL AuNRs, 0.25 mL of 0.10 M H_2O_2, 0.30 mL of 1.0 M HCl and 0.20 mL Fe^{3+} of different concentrations were added to a 10.0-mL colorimetric tube and diluted to 10.0 mL with water. After quick mixing, the solution was incubated at 70 °C for 25 min and then put on ice-water for 5 min to stop the reaction completely. The reagent blank experiment was also carried out. Absorption spectra of the system were scanned and the LPAB of test solution (λ_2) and reagent blank (λ_1) were recorded, respectively, and the blue shift ($\Delta\lambda=\lambda_1-\lambda_2$) was calculated.

3. Results and discussion

3.1. Sensing mechanism

As shown in Fig. 1, the initial AuNRs exhibit two plasmon absorption bands located at 716 nm for LPAB and at 520 nm for TPAB, respectively (Fig. 1, curve a); no obvious change was found in absorption spectra of AuNRs in the presence of H_2O_2 ($\Delta\lambda=6$ nm, $\Delta A=0.007$, Fig. 1, curve b); while the blueshift of LPAB was observed with decrease of the corresponding absorbance after adding HCl ($\Delta\lambda=34$ nm, $\Delta A=0.105$, Fig. 1, curve c).

There are two possible reasons for these phenomena: on the one hand, because of the standard electron potential of H_2O_2/H_2O (E=1.776 V) is higher than that of Au (III)/ Au (0) ($E=1.500$ V) [25] at pH 1.55, resulting AuNRs were oxidized to AuNRs' by H_2O_2 (Scheme 1 a); on the other hand, the standard electron potential of Au (III)/ Au (0) ($AuCl_4^-$/Au (0), E=1.002 V) decreased because of the complexation of Cl^- ions in HCl with Au [20], showing that Cl^- had activating effect on the oxidation reaction between H_2O_2 and AuNRs. Besides, the blueshift of LPAB could be explained as H_2O_2 oxidized selectively the tips of AuNRs due to the shielding effects of the surfactant CTAB mainly covering on the transverse sides of AuNRs [19], caused the aspect ratio of AuNRs to decrease [26].

When Fe^{3+} was added in the AuNRs–H_2O_2–HCl system, the increasing of Fe^{3+} concentration caused the $\Delta\lambda$ of the LPAB to increase and the corresponding absorbance of the LPAB to decrease (Fig. 2), as well as the color of the solution to change obviously (Fig. 3). The phenomenon could be explained as Fe^{3+} had strong catalytic effect on the oxidation reaction between H_2O_2

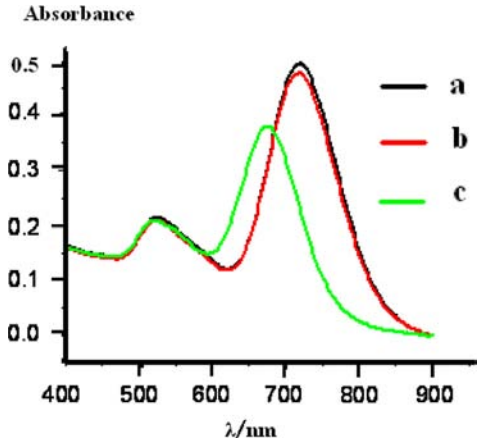

Fig. 1. UV–vis absorption spectra of AuNRs–H_2O_2–HCl system (The component of each curve presents as follows: (a): 0.75 mM AuNRs, (b): a+2.5 mM H_2O_2, and (c): b +30 mM HCl. The experiment was carried out at 70 °C for 20 min and pH was 1.55).

a

$$AuNRs + H_2O_2 + 2H^+ \rightarrow AuNRs' + 2H_2O$$

b

$$Fe^{3+} + H_2O_2 \rightarrow Fe^{2+} + OOH\bullet + H^+$$

$$Fe^{2+} + H_2O_2 \rightarrow Fe^{3+} + OH\bullet + OH^-$$

c

$$AuNRs + OOH\bullet + H^+ \rightarrow AuNRs' + 2H_2O$$

$$AuNRs + OH\bullet + H^+ \rightarrow AuNRs' + 2H_2O$$

Scheme 1. Sensing mechanism for the determination of Fe^{3+}. (a) Reaction between H_2O_2 and AuNRs (b) Fenton reaction (c) Reaction of OOH• and OH• oxidation AuNRs.

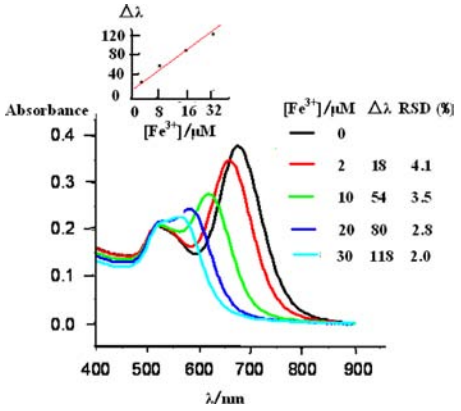

Fig. 2. UV–vis absorption spectra of AuNRs–H_2O_2–HCl–Fe^{3+} system containing 0.75 mM AuNRs, 2.50 mM H_2O_2, 30.0 mM HCl and different concentrations of Fe^{3+} at 70 °C for 25 min under pH 1.55. Inset: working curve of the $\Delta\lambda$ vs the concentration of Fe^{3+}.

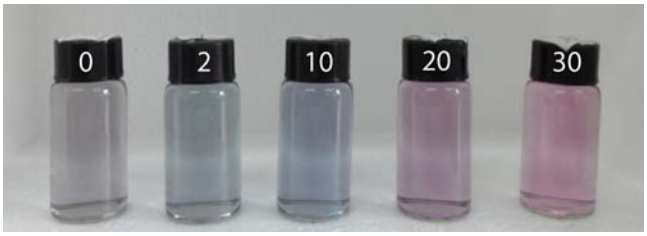

Fig. 3. Color responses when 0.75 mM AuNRs react with Fe^{3+} (from left to right: 0, 2, 10, 20, 30 μM) system containing 2.50 mM H_2O_2 and 30.0 mM HCl at 70 °C for 25 min under pH 1.55.

and AuNRs. When the concentration of Fe^{3+} was 30.00 μM, the $\Delta\lambda$ of system was 3.5 times (118 nm/34 nm) larger than that of uncatalyzed reaction, showing the Fe^{3+} had signal amplification effect on the $\Delta\lambda$ of system. More interestingly, the LPAB gradually blueshifted and absorbance decreased with the increasing of [Fe^{3+}], resulting in that plasmon absorption bands located at 558 nm for TPAB, which was like with the UV–vis absorption spectra of Au nanospheres at 520 nm [25]. Thus, we could conclude that the gold nanostructures changed from rods (Fig. 4 a) to spheres (Fig. 4 b) gradually. With the evolution of the catalytic effect of Fe^{3+} on the reaction of H_2O_2 oxidizing AuNRs, the aspect ratio of AuNRs decrease and the LPAB blueshifted gradually. What's more, the $\Delta\lambda$ of system was linear to the concentration of Fe^{3+} in the range of 0.20–30.0 μM (Fig. 2, inset), allowing determination of Fe^{3+} using AuNRs as catalyzing non-aggregation colorimetric sensor.

Reaction between H_2O_2 and AuNRs (Scheme 1 a) was shown as follows:

When Fe^{3+} was added in the AuNRs–H_2O_2–HCl system, Fe^{3+} could react with H_2O_2 to form Fe^{2+} and OOH•, and then Fe^{2+} reacted with H_2O_2 to form Fe^{3+} and OH• (Scheme 1 b):

The OOH• and OH• oxidized AuNRs to AuNRs' because of strong oxidization capability (Scheme 1 c)

Schematic illustration for the designed catalyzing non-aggregation colorimetric sensor for Fe^{3+} detection was showed as Scheme 2.

In order to prove the probability of sensing mechanism for the determination of Fe^{3+}, the structures of AuNRs were characterized. Representative TEM images of AuNRs in AuNRs–H_2O_2 system (Fig. 4a) and AuNRs–H_2O_2–Fe^{3+} system (Fig. 4b) revealed the presence of clearly defined features of an average size of ~40 nm (rod state) and 10 nm (sphere state), respectively, because of oxidizing speed of Fe^{3+} catalyzing H_2O_2 to oxidize AuNRs was fast, caused the aspect ratio of AuNRs to sharply decrease. These facts above not only confirmed the catalysis of Fe^{3+} on oxidation reaction between the H_2O_2 and AuNRs, but also demonstrated the probability of sensing mechanism for the determination of Fe^{3+}.

3.2. Optimization of experimental conditions

For the system containing 10.0 μM Fe^{3+}, a number of parameters that influence on the sensitivity, selectivity, accuracy and stability of the sensor were investigated in a univariate approach.

3.2.1. Effects of the concentration of AuNRs and H_2O_2

The concentration of nanorods was estimated by assuming a 100% synthetic yield [19]. The effects of the concentration of AuNRs and H_2O_2 on the $\Delta\lambda$ of the system were examined, respectively. Low concentration of AuNRs and H_2O_2 narrowed linear range, while high concentration caused sensitivity to lower. As show in Fig. 5, the $\Delta\lambda$ of system enhanced with the increasing of the concentration of AuNRs, while the $\Delta\lambda$ of system reached the peak value at 0.75 mM and kept almost invariant when exceed 0.75 mM; when the concentration of AuNRs was 0.75 mM, the $\Delta\lambda$ of system enhanced with the increasing of the concentration of H_2O_2, while the $\Delta\lambda$ of system reached the peak value at 2.50 mM and the $\Delta\lambda$ of system decreased when exceed 2.50 mM. In consideration of both linear range and sensitivity, 0.75 mM AuNRs and 2.50 mM H_2O_2 were chosen as the optimal concentration.

3.2.2. pH of the system

Bcause of Fe^{3+} easily was hydrolyzed resulting in the formation of $Fe(OH)_3$ under alkaline conditions, thus HCl was used to control pH of the system. As shown in Fig. 5, the $\Delta\lambda$ of system was 0, and the $\Delta\lambda$ of system increased until the concentration of HCl reached 30.0 mM (pH 1.55) when the pH of the solution was 2.33. The phenomena were attributed to the formation of $AuCl_4^-$ which caused the potential of Au (III)/Au (0) to decrease [20], and was favored to the reaction that Fe^{3+} catalyzing H_2O_2 to oxidize AuNRs. When the pH of the system was 1.55, the $\Delta\lambda$ of system reached the maximum and kept constant when the pH of the system was less than 1.55. The reason for the phenomena was that the catalytic reaction completed and AuNRs changed from rods to spheres, resulting in the response of sensor to Fe^{3+} declined gradually. Therefore, the optimum pH of the system was 1.55.

3.2.3. Effects of reaction temperature and time

The effects of the temperature and time on the $\Delta\lambda$ of the system were investigated. When the reaction temperatures were 40, 50, 60, 70 and 80 (°C), the $\Delta\lambda$ of system were 2, 10, 16, 54 and 36 (nm), the corresponding RSD (%) were 4.9, 4.0, 3.7, 1.2 and 2.6,

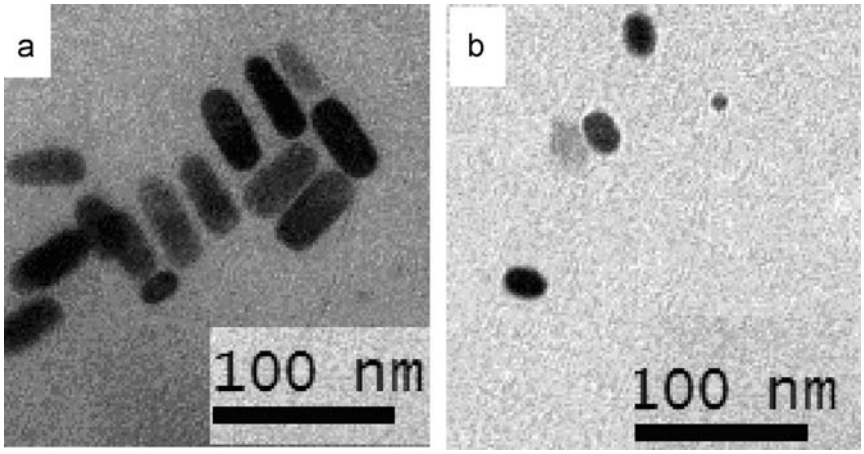

Fig. 4. (a) TEM image of AuNRs in AuNRs-H_2O_2 system and (b) TEM image of AuNRs in AuNRs–H_2O_2–Fe^{3+} system.

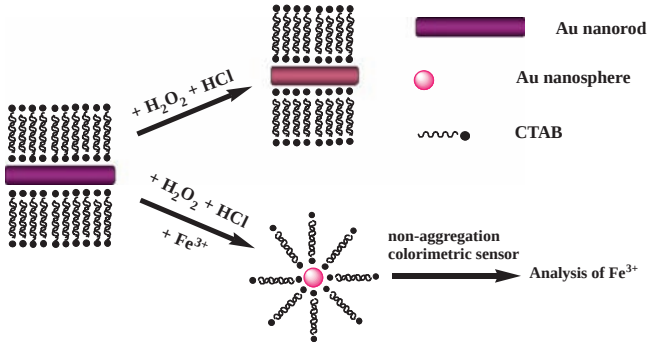

Scheme 2. Sensing mechanism for the determination of Fe^{3+}.

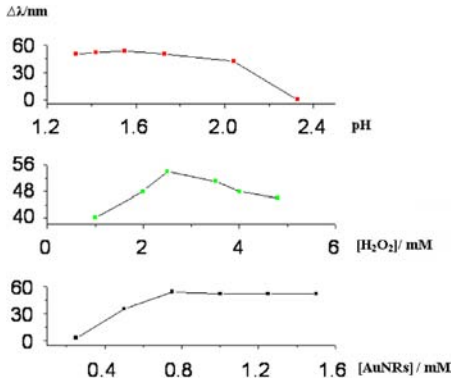

Fig. 5. Effect of pH, the concentration of AuNRs and H_2O_2 on the $\Delta\lambda$ of the system (The experimental concentration: containing 10.0 μM Fe^{3+} and at 70 °C for 25 min.).

respectively. Results show that the $\Delta\lambda$ of system increased with the increasing of reaction temperature and reached the maximum at 70 °C; when the temperature exceeded 70 °C, the $\Delta\lambda$ of system decreased. This could be explained as that the decomposition of H_2O_2 at high temperature was against the catalytic reaction to carry out. At the same time, when the reaction time were 5, 10, 15, 20 and 25, 30 (min), the $\Delta\lambda$ of system were 7, 15, 29, 43, 56 and 54 (nm), the corresponding RSD (%) were 4.4, 3.6, 3.4, 2.4, 1.0 and 1.2, respectively. Results show that the $\Delta\lambda$ of system increased gradually with the increasing of the reaction time and reached the maximum at 25 min. The $\Delta\lambda$ of system remained stable in 25 min after being cooled in ice water for 5 min (data are not shown), showing the good stability of non-aggregation colorimetric sensor. Thus, 70 °C and 25 min were chosen as the optimal reaction condition.

3.3. Selectivity of the sensor

To evaluate the selectivity of sensor towards the sample containing 10.0 μM Fe^{3+}, a series of coexistent ions in human serum were investigated under the optimum measurement conditions. When the relative error (Er) exceeded ± 5%, each ion is considered as interfering agent. Results show that the allowable concentrations of most ions are high: 1000 μM for K^+, Na^+, Mg^{2+}, Ca^{2+}, Mn^{2+}, Co^{2+} and Pb^{2+} as well as 500.0 μM for Ni^{2+}, showing that this sensor has excellent selectivity.

3.4. Working curve, linear range and LOD

Under the optimum conditions, the Δλ of the system was linear with the concentration of Fe^{3+} in the range of 0.20–30.0 μM, the regression equations was $\Delta\lambda = 11.52 + 3.704\ [Fe^{3+}]$ (μM), correlation coefficients (r) was 0.9949 ($n=6$). The RSD (%, $n=6$) were 4.8 for 0.20 μM and 2.1 for 30.0 μM, respectively. The LOD was 0.067 μM (calculated by 3 Sb/k, here Sb represents the standard deviation of 11 blank measurements and the value was 0.0083, k is the slope of standard curve), showing the higher sensitivity and wider linear range of the sensor than those in Ref. [15] (The LOD is 5.6 μM. The linear range is 10–60 μM.). There are two reasons for higher sensitivity of this sensor. Firstly, the complexation of Cl^- ions in HCl with Au reduced the standard electron potential of Au (III)/Au (0) [20], showing that Cl^- had activating effect on the reaction of H_2O_2 oxidizing AuNRs; Secondly, the catalytic effect of Fe^{3+} on the reaction of H_2O_2 oxidizing AuNRs greatly improved $\Delta\lambda$ value [27], showing the signal amplification of catalytic reaction.

3.5. Analytic application

0.10 mL blood sample was taken and added 0.30 mL mixed acid (HCl: HNO_3 = 1:1), incubated the solution at 120 °C for 30 min, and then kept in ice-water bath for 5 min. Then, the solution was diluted to μM level by Triton X-100-HCl (The mixing solution of 0.50 mL Triton X-100 and 0.50 mL HCl was diluted to 1000 mL with water.) for use. 1.00 mL test solution was taken and the content of Fe^{3+} was determined according to the experimental method. Standard addition recovery experiment was simultaneously conducted. This method was compared with ICP–MS. The results are listed in Table 1.

Seen from Table 1, in the case of serum A, B, C, D, E, F, G, and H, the F was 1.27, 2.22, 1.56, 1.28, 2.30, 2.07, 1.97 and 2.76, respectively, indicating that there was no significant differences between S_1 and

Table 1
Results of the detection of Fe^{3+} in blood samples and its analysis of the significant differences ($P=90\%$, $f=n_1+n_2-2=9$, $F_{0.95,9}=6.3$, $t_{0.90,9}=1.8$).

Blood samples	The method ($n=6$)			ICP–MS ($n=5$)			Statistical analysis		
	Measured value (μM)	$\overline{X}_1$ (μM)	S_1	Measured value (μM)	$\overline{X}_2$ (μM)	S_2	F	$\overline{S}$	t
A	4980.12, 4985.21, 4984.33, 4995.37, 4983.46, 4987.66,	4986.03	5.20	4979.63, 4984.36 4974.42, 4990.27 4982.38	4982.21	5.85	1.27	5.53	1.14
B	6978.32, 6982.23, 6973.27, 6979.16, 6979.65, 6985.47	6979.68	4.08	6981.42, 6985.24, 6978.45, 6982.67 6984.71,	6982.50	2.74	2.22	3.41	1.80
C	8760.67, 8764.24, 8755.34, 8759.19, 8752.81, 8756.92	8758.20	4.06	8764.54, 8769.45, 8759.23, 8764.41 8756.47,	8762.82	5.07	1.56	4.57	1.67
D	10204.45, 10207.73, 10208.61, 10213.73 10206.44, 10211.81	10208.80	3.44	10201.75, 10204.66 10206.83, 10209.75 10203.91	10205.38	3.04	1.28	3.24	1.74
E	2560.34, 2563.47, 2564.25, 2559.16, 2562.81, 2561.42,	2561.91	1.95	2562.85, 2566.55 2567.76, 2560.32 2564.28	2564.35	2.96	2.30	2.46	1.64
F	2634.51, 2639.61, 2629.56, 2633.87, 2625.77, 2630.92,	2632.37	4.75	2629.17, 2633.71, 2625.33, 2627.72 2631.78	2629.54	3.30	2.07	4.02	1.16
G	3072.47, 3076.54, 3075.31, 3073.75 3074.66, 3070.86	3073.93	2.04	3073.63, 3068.36 3069.47, 3075.24 3070.94	3071.53	2.86	1.97	2.45	1.62
H	3463.29, 3459.92, 3467.35, 3454.37 3464.83, 3458.77	3461.42	4.67	3461.89, 3465.63 3463.45, 3460.71 3467.38	3463.87	2.81	2.76	3.74	1.08

S_2, and the corresponding t was 1.14, 1.80, 1.67, 1.64, 1.16, 1.62 and 1.08, respectively, indicating that there was also no significant differences between $\overline{X}_1$ and $\overline{X}_2$. Besides, compared with the ICP–MS, the relative error of the detection results was less than $\pm 5\%$, indicating this sensor has high accuracy. The amount of Fe^{3+} in serum of healthy human is in the range of 4200–11000 μM, while that in serum of diabetes suffer is less than 4200 μM. Thus, we can diagnose that A–D are of healthy human, E–H are those who suffer from diabetes, revealing that the sensor possess important clinical application.

4. Conclusions

In this work, a catalyzing non-aggregation colorimetric sensor with signal amplification for the determination of Fe^{3+} has been proposed based on the fact that Fe^{3+} could accelerate the reaction between AuNRs and H_2O_2, caused rapid response of the $\Delta\lambda$ to [Fe^{3+}]. This rapid, simple, sensitive and selective sensor without surface modification not only displays potential application prospect in metal ion analysis, but also indicates notable advantage of combination between high sensitivity of non-aggregation colorimetric sensor and signal amplification of catalytic reaction and effectively promoted the development and applications of the AuNRs, colorimetric sensors and catalytic kinetic analysis.

Acknowledgments

This work was supported by the Fujian Province Natural Science Foundation (Grant no. 2010J01053, 2009J1017 and 2008J0313), the Fujian Province Education Committee (A10277, JA08252, JB08262 and JB09278), the Fujian Provincial Bureau of Quality and Technical Supervison (FJQI 2011006) and the Scientific Research Program of Zhangzhou Institute of Technology Foundation (ZZY1215, ZZY 1007 and ZZY1009). At the same time, we are very grateful to precious advices raised by the anonymous reviewers.

References

[1] D. Yuan, D.Y. Fu., Anal. Lett. 44 (2011) 271–283.
[2] J.E.T. Andersen, Analyst 130 (2005) 385–390.
[3] C.M.G. van den Berg., Anal. Chem. 78 (2006) 156–163.
[4] M.E del Castillo Busto, M. Montes-Bayon, E. Blanco-Gonzalez, J. Meija, A. Sanz-Medel., Anal. Chem. 77 (2005) 5615–5621.
[5] G.L. Arnold, S. Weyer, A.D. Anbar., Anal. Chem. 76 (2004) 322–327.
[6] K. Pomazal, C. Prohaska, I. Steffan, G. Reich, J.F.K. Huber, Analyst 124 (1999) 657–663.
[7] H. Beitollahi, J.B. Raoof, R. Hosseinzadeh., Talanta 85 (2011) 2128-2134.
[8] H. Beitollahi, H. Karimi-Maleh, H. Khabazzadeh., Anal. Chem. 80 (2008) 9848–9851.
[9] H. Beitollahi, J.B. Raoof, H. Karimi-Maleh, R. Hosseinzadeh., J. Solid State Electrochem. 16 (2012) 1701–1707.
[10] S. Salmanpour, T. Tavana, A. Pahlavan, M.A. Khalilzadeh, A.A. Ensafi, H. Karimi-Maleh, H. Beitollahi, E. Kowsari, D. Zareyee, Mat. Sci. Eng. C 32 (2012) 1912–1918.
[11] T. Tavana, M.A. Khalilzadeh, H. Karimi-Maleh, A.A. Ensafi, H. Beitollahi, D. Zareyee, J. Mol. Liq. 168 (2012) 69–74.
[12] A. Mokhtari, H. Karimi-Maleh, A.A. Ensafic, H. Beitollahi, Sensor. Actuat. B 169 (2012) 96–105.
[13] M. Keyvanfard, R. Shakeri, H. Karimi-Maleh, K. Alizad., Mat. Sci. Eng. C 33 (2013) 811–816.
[14] M. Baghayeri, M. Namadchian, H. Karimi-Maleh, H. Beitollahi., J. Electroanal. Chem. 697 (2013) 53–59.
[15] S.P. Wu, Y.P. Chen, Y.M. Sung, Analyst 136 (2011) 1887–1891.
[16] Z.L. Jiang, S.J. Sun, A.H. Liang, W.X. Huang, A.M. Qin., Clin. Chem. 52 (2006) 1389–1394.
[17] X.L. Ren, L.Q. Yang, J. Ren., Nanoscale Res. Lett. 5 (2010) 1658–1663.
[18] L.M. Liz-Marzán., Langmuir 22 (2006) 32–41.
[19] M. Rex, F.E. Hernandez, A.D. Campiglia., Anal. Chem. 78 (2006) 445–451.
[20] F.M. Li, J.M. Liu, X.X. Wang, L.P. Lin, W.L. Cai, Y.N. Zeng, L.H. Zhang, S.Q. Lin., Sensor. Actuat. B. Chem. 155 (2011) 817–822.
[21] N. Xiao, C.X. Yu., Anal. Chem. 82 (2010) 3659–3663.

[22] P.K. Sudeep, S.T. Shibu Joseph, K.G. Thomas., J. Am. Chem. Soc. 127 (2005) 6516–6517.
[23] C.V. Durgadas, V.N.L.C.P. Sharma, K. Sreenivasan., Sensor. Actuators. B. Chem 156 (2011) 791–797.
[24] B. Nikoobakht, M.A. El-Sayed., Chem. Mater. 15 (2003) 1957–1962.
[25] C.K. Tsung, X.S. Kou, Q.H. Shi, J.P. Zhang, M.H. Yeung, J.F. Wang, G.D. Stucky., J. Am. Chen. Soc. 128 (2006) 5352–5353.
[26] J. Chang, H. Wu, H. Chen, Y. Ling, W. Tan., Chem. Commun. 8 (2005) 1092–1094.
[27] C. Walling, A. Goosen., J. Am. Chem. Soc. 95 (1973) 2987–2991.